nature microbiology

ARTICLES

https://doi.org/10.1038/s41564-020-00851-2

Niche dimensions of a marine bacterium are identified using invasion studies in coastal seawater

Brent Nowinski and Mary Ann Moran ✉

Niche theory is a foundational ecological concept that explains the distribution of species in natural environments. Identifying the dimensions of any organism's niche is challenging because numerous environmental factors can affect organism viability. We used serial invasion experiments to introduce *Ruegeria pomeroyi* DSS-3, a heterotrophic marine bacterium, into a coastal phytoplankton bloom on 14 dates. RNA-sequencing analysis of *R. pomeroyi* was conducted after 90 min to assess its niche dimensions in this dynamic ecosystem. We identified ~100 external conditions eliciting transcriptional responses, which included substrates, nutrients, metals and biotic interactions such as antagonism, resistance and cofactor synthesis. The peak bloom was characterized by favourable states for most of the substrate dimensions, but low inferred growth rates of *R. pomeroyi* at this stage indicated that its niche was narrowed by factors other than substrate availability, most probably negative biotic interactions with the bloom dinoflagellate. Our findings indicate chemical and biological features of the ocean environment that can constrain where heterotrophic bacteria survive.

Heterotrophic bacteria have important roles in the Earth's carbon and nutrient cycles, shaping natural and human ecosystems through their metabolic and ecological functions. In the ocean, bacteria mediate flux between major carbon reservoirs, control nutrient availability and participate in marine food webs. Many environmental factors govern these activities, including seawater mixing, photosynthetically active irradiance levels[1,2], organic resources[3], nutrients[3,4], and mutualistic and antagonistic interactions with other species[5,6]. These factors form the dimensions of each bacterial species' niche, a foundational ecological concept in which the abiotic and biotic variables that influence the birth and death rates of a species determine where it can exist in nature[7,8].

Identifying the dimensions of marine bacterial niches promises to improve understanding and predictability of the processes that drive ocean biogeochemistry. Hutchinson defined the 'fundamental' niche as the full range of external conditions in which an organism is viable (that is, has an intrinsic growth rate, r_0, ≥ 0) in the absence of interference from biotic interactions, and the 'realized' niche as the fundamental niche in the presence of other species. The realized niche is typically considered to be a more restricted ecological space than the fundamental niche due to negative interactions with competitors and predators[8]. Although the niche concept has long been a useful framework[9,10], the myriad possible environmental influences controlling ecological success of a species makes comprehensive analyses of niche dimensions difficult in practice. For marine bacteria, selected niche dimensions have been addressed by correlations to environmental factors[11] and growth responses under defined laboratory conditions[12]. As basic rules of marine bacterial ecology are still being discovered, however, untargeted methodologies—those not limited to preselected factors—provide a more inclusive accounting of features determining a bacterium's viability.

Shifts in bacterial messenger RNA pools in situ represent untargeted proxies for the realized niche dimensions invoking bacterial sensing and phenotypic response[13–15]. In complex ecosystems, transcripts drawn simultaneously from multiple community members make it challenging to characterize niche dimensions of coexisting taxa. Mapping transcripts to genomes assembled from single cells or community sequencing parses the aggregated response[16,17], although these reference genomes are typically incomplete and, when derived from metagenomic data, can blur responses through aggregation of multiple populations[18]. The extent to which environmental stimuli are manifested in transcriptomes also differs among taxa, with bacteria that harbour few regulatory elements exhibiting only minor transcriptional shifts compared with those with well-regulated genomes experiencing identical perturbations[14,19].

In the present study, we aim to characterize bacterial niche dimensions using a variation of an invasion study, an approach typically used to address ecological principles governing the outcome of invasion of an existing community by a foreign species[20,21]. Our variation made experimental invasions of a heterotrophic marine bacterium into an existing community to identify factors that make up the bacterium's niche dimensions. Unlike in metatranscriptomic surveys, the genetic background and physiological state of the bacterium before introduction were standardized, providing the advantage of a single, well-characterized organism typical of model system studies, yet capturing the complexity of natural ecosystems. Over a 5-week period, the metabolically responsive marine bacterium *R. pomeroyi* DSS-3 was added into surface seawater samples from Monterey Bay, in California (the 'introduction' step of the invasion[21]). The additions occurred during the progression of a massive bloom of the dinoflagellate *Akashiwo sanguinea*[22], an ecologically relevant situation for *R. pomeroyi* given its cultivation from coastal waters where *A. sanguinea* occurs[23–25]. Transcriptome analysis of the invading bacterium was conducted after 90 min to identify the abiotic and biotic factors of the shifting bloom that triggered phenotypic responses (the 'establishment' stage of the invasion)[21]. We report untargeted analyses of the dynamic factors affecting the viability of a heterotrophic bacterium, the life history strategy of which is tied to marine microphytoplankton[26].

Department of Marine Sciences, University of Georgia, Athens, GA, USA. ✉e-mail: mmoran@uga.edu

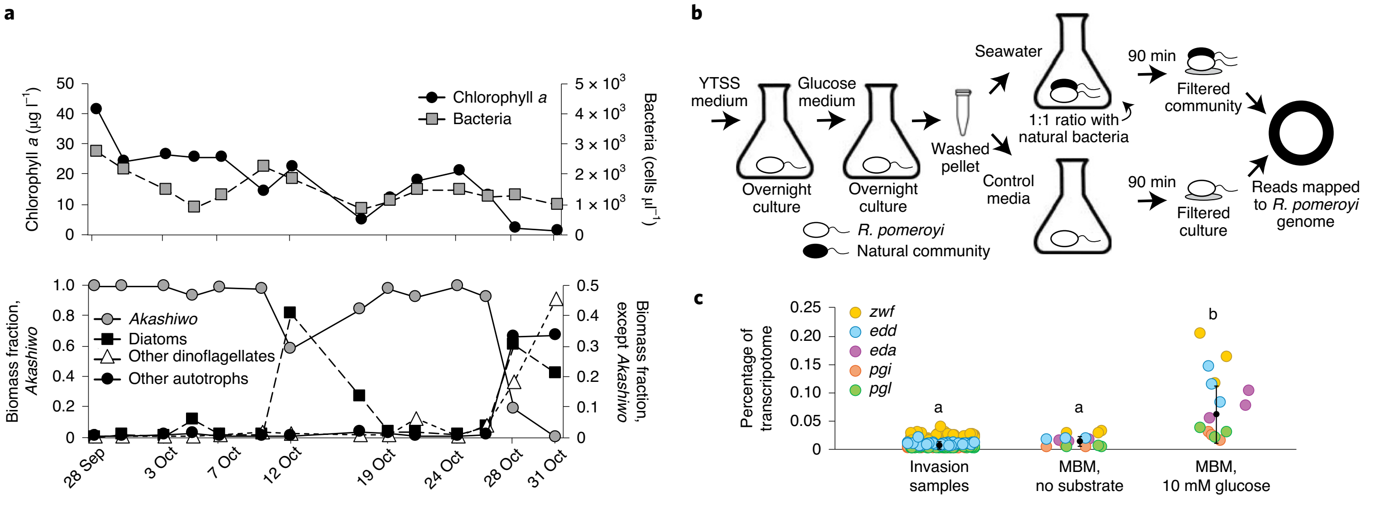

Fig. 1 | Conditions and methods for invasion studies. **a**, Chemical and biological features of the 2016 Monterey Bay autumn bloom. Top panel: Chl *a*, $n = 3 \pm 1$ s.d. (error bars fall within the symbols); bacterial cell counts, $n = 2$. Bottom panel: $n = 1$. Note that different scales are used on the left and right axes of the bottom panel. **b**, Protocol for invasion experiments carried out for three independent biological replicates. **c**, Relative expression of five *R. pomeroyi* glucose catabolism genes in 14 invasion studies compared with controls incubated in MBM without a substrate or with glucose. Small black symbols and error bars represent the mean ± 1 s.d. Treatments differ significantly from each other (analysis of variance $P < 0.0001$, d.f. = 2), with different lower case letters indicating significant differences in post-hoc analysis (two-sided Tukey's honestly significant difference; $P = 0.0010$ for MBM glucose versus invasion studies and $P = 0.0010$ for MBM + glucose versus MBM with no substrate).

Results

Invasion manipulation. The surface waters of Monterey Bay, in California, hosted a large bloom of the dinoflagellate *A. sanguinea* in the autumn of 2016 with chlorophyll *a* (Chl *a*) levels >50 µg l^{-1} (ref. [22]). The gene sequencing of 18S ribosomal RNA showed the protist community shifting over the study period to a mixture of diatoms and dinoflagellates, including dinoflagellate parasites. *A. sanguinea* accounted for >99% of phytoplankton biomass in late September but <20% in late October (Fig. 1a and Extended Data Fig. 1). A rapid decrease of *A. sanguinea* biomass in mid-October highlighted a distinct water mass moving through the sampling station, evident from salinity and temperature shifts (Extended Data Fig. 2).

On 14 dates over 5 weeks, the heterotrophic marine bacterium *R. pomeroyi* was pre-grown under a standard protocol and introduced into bloom seawater (Fig. 1b; $n = 3$) to approximate a 1:1 ratio of introduced:native bacteria. After incubation under identical temperature (24 °C) and light (ambient laboratory) conditions for 90 min, the seawater transcriptome was sequenced, with *R. pomeroyi* accounting for $48.5 \pm 13.4\%$ of bacterial mRNA reads (Supplementary Table 1). The sensitivity of *R. pomeroyi* to ecological signals under this invasion protocol was assessed by preparing cells as for the field samples, but inoculating into defined minimal medium with 10 mM glucose or without substrate (Fig. 1b). These controls verified robust *R. pomeroyi* expression responses 90 min post-introduction and confirmed gene expression responses consistent with medium conditions (Fig. 1c). Principal component analysis (PCA) of genome-wide expression patterns indicated that the *R. pomeroyi* profiles from the bloom diverged from those in defined medium and were distinctly non-random. Transcriptome composition largely tracked with the date of sample collection (Fig. 2a) and shifts in protist community composition (Fig. 2b). A growth rate index for *R. pomeroyi* (ribosomal protein transcript abundance as percentage of transcriptome) was elevated in glucose controls (9.6%) compared with no-glucose controls (3.0%), and was lowest in the seawater invasion experiments (1.0–2.7%).

Gene expression patterns. The 4,278 protein-encoding genes in the *R. pomeroyi* genome were categorized into 17 expression modules based on transcriptional patterns across the 14 independent introductions to bloom seawater (Fig. 2c). The largest module contained 1,417 genes with maximum relative expression in the initial samples corresponding to the peak of the bloom and decreases as the bloom aged (turquoise module); four additional modules positively correlated with this module (Pearson's $r = 0.70–0.98$, $P < 0.01$, degrees of freedom (d.f.) = 12) were merged to create a supermodule of 2,087 genes with the highest expression in the peak-bloom stages. The second largest module contained 915 genes with the opposite pattern—minimum relative expression under peak-bloom conditions and increases over time (orange module); two additional modules that positively correlated with this module ($r = 0.75$ and 0.76; $P < 0.01$) were merged to create a supermodule of 1,423 genes with expression maxima in the late-bloom stages (Fig. 2c). Together, the two supermodules accounted for 82% of the *R. pomeroyi* genome (49% peak-bloom and 33% late-bloom genes) and were negatively correlated with each other (Pearson's $r = -0.91$, $P < 0.001$, d.f. = 12). Genes with maxima during the peak bloom correlated positively with *A. sanguinea* biomass and Chl *a* concentration; late-bloom genes correlated positively with diatom biomass and a dinoflagellate parasite (Extended Data Fig. 3).

Niche dimension analysis. We considered the aspects of niche theory that can be informed by sequential microbial invasion experiments. Hutchinson[8] defined the niche as the conditions in a specific geographical space that allow an organism to 'survive and reproduce'[27], a criterion formalized as an intrinsic growth rate ≥0 (ref. [28]). Although niches are genetically determined[29,30], neither a genome nor a transcriptome can delineate the Hutchinsonian niche because neither indicates whether growth is possible under existing conditions. For example, genomic data might indicate a microbe's capability of metabolizing a substrate, but not whether the supply of this substrate is sufficient to support growth. Genomes and transcriptomes do, however, indicate niche dimensions—the factors that influence a species' growth in a given environmental space; genomes provide insights into the functions an organism could invoke in reaction to a dimension, and transcriptomes indicate whether these functions are currently invoked[31]. Niche theory also

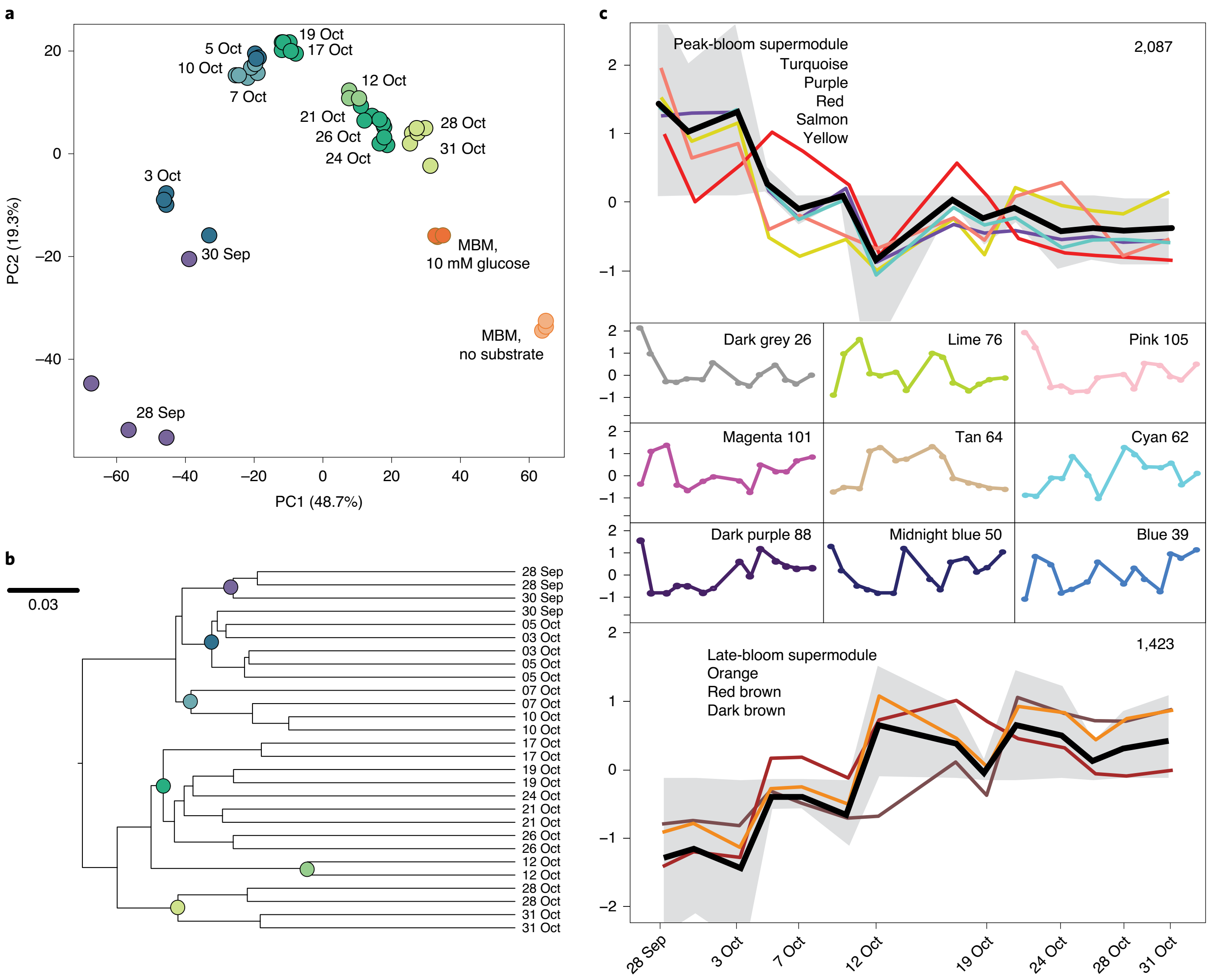

Fig. 2 | *R. pomeroyi* gene expression patterns in Monterey Bay invasion studies. a, PCA of whole transcriptome expression patterns in invasion and control experiments. The 14 invasion experiments are labelled by date ($n = 3$ except for 30 September where $n = 2$). **b**, The symbols are coloured based on UPGMA UniFrac clustering of 18S rRNA gene sequences from the protist communities (Extended Data Fig. 1). Colours at clade nodes indicate the corresponding sample date in **a**. **c**, *R. pomeroyi* genes classified based on expression patterns over the 14 invasion experiments. Significantly correlated modules were merged into peak-bloom or late-bloom supermodules. Data are mean *z*-scores ($n = 3$ except for 30 September where $n = 2$). Numbers in the upper right corner indicate the gene counts in each module/supermodule. Black lines are the average of all genes in the supermodules and grey shading is the s.d. of the mean value.

distinguishes between the ‘fundamental’ and ‘realized’ niches[8], the former referring to the conditions in which a species grows without consideration of interference from other organisms, and the latter to the (typically narrower) set of conditions in which a species grows in the presence of other organisms, reflecting the outcome of competition for substrates or space, for example. Invasion experiments in which introductions are made into intact natural systems, as done here, include dimensions imposed by biotic interactions and therefore address realized niche dimensions of the invader.

The realized niche dimensions influencing the viability of *R. pomeroyi* in the Monterey Bay phytoplankton bloom in the autumn of 2016 were operationally defined from the functional annotation of genes with significant relative expression changes through time. We focused first on the 3,510 genes of the peak- and late-bloom supermodules because of their clear temporal patterns. A statistically significant difference in relative expression between the two initial and two final time points was considered a measurable transcriptional response to an environmental signal (DeSeq2, adjusted $P < 0.05$) and was found for 1,382 genes. Of *R. pomeroyi* genes, 18% were not included in the supermodules. For these, a statistically significant difference in relative expression between the two highest and the two lowest time points was considered a measurable response to an environmental signal, and was found for 423 genes.

Chemical niche dimensions. Invasions into the phytoplankton bloom identified at least 43 substrate-based niche dimensions for *R. pomeroyi*, recognized from transcriptional responses of genes transporting organic molecules supporting growth. Another 13 potential substrate dimensions were suggested from transcriptional response of genes catabolizing organic molecules, although these are potentially counted among the transporters that lack definitive substrate annotations. Nitrogen-containing compounds made up a surprising 67% of the substrate-based niche dimensions (29 compounds), and all but two invoked the highest expression levels during invasions of the *A. sanguinea*-dominated peak bloom (Fig. 3). Peak-bloom, nitrogen-containing substrate dimensions included *N*-methyl compounds (trimethylamine *N*-oxide, carnitine, choline, glycine betaine), amino acids and related molecules (polyamines, peptides), and sulfonated organic nitrogen compounds (taurine, *N*-acetyltaurine, cysteate). Two N-containing substrate dimensions elicited the highest expression later in the bloom (ectoine and a putative branched-chain amino acid; Fig. 3). *R. pomeroyi* reacted to five sulfur-containing substrates, including the three sulfonated nitrogen compounds above plus dimethylsulfoniopropionate (DMSP) and isethionate; these also elicited the strongest responses when the bacterium invaded peak-bloom samples. Niche dimensions based on organic compounds with carbon-only backbones included the C1 molecules carbon monoxide and formate, six carboxylic acids including lactate, three sugars including ribose, and the aromatic compounds ferulate, catechol and protocatechuate (Fig. 3 and Supplementary Table 2); again, *R. pomeroyi* reacted to these most strongly during the peak bloom. The carbon-only compounds with highest influence in late-bloom samples were those processed through the ethylmalonyl-CoA pathway for C2 substrate catabolism. Ramping up of carbon storage as polyhydroxybutanoate in the late bloom indicated that organic carbon accumulation in the bloom environment was relevant to *R. pomeroyi*'s ecological success (Fig. 3).

Other chemical dimensions of *R. pomeroyi*'s niche in the Monterey Bay bloom were related to nutrient and metal concentrations. The bacterium had high uptake responses for ammonium and urea at the earliest two sample dates, suggesting nitrogen limitation during the peak bloom[32] (Fig. 3). *A. sanguinea* biomass was positively correlated with expression of these genes (Pearson's $r = 0.95$, $P < 0.01$, d.f. = 12; Extended Data Fig. 4) and, given the dinoflagellate's high affinity for inorganic nitrogen and preference for ammonium[33], probably drew down nitrogen concentrations at the bloom peak. Indeed, *R. pomeroyi* cannot assimilate nitrate and relies on ammonium for inorganic nitrogen[34]. *R. pomeroyi* also differentially expressed genes for acquisition of sulfate, phosphonate and phosphate (Fig. 3). Bacterial initiation of phosphorus storage in the late-bloom environment pointed to phosphate availability as an important niche dimension. *R. pomeroyi* responded to the availability of four metals, increasing expression for magnesium transport when introduced into the peak bloom, and for manganese, iron and zinc transport later on (Fig. 3).

Biotic interaction niche dimensions. On about half the invasion dates, a feature of the environment induced *R. pomeroyi* to synthesize indole acetic acid, a molecule enhancing growth of co-occurring phytoplankton[35]. On two dates, *R. pomeroyi* ramped up transcription of genes encoding a diffusible killing mechanism that targets diverse bacterial taxa[36] (Fig. 3). The specific dimensions that drive transcription of these non-trophic biotic interaction genes after 90 min in the bloom are likely to include specific protist or bacterial taxa in the invaded microbial community (Extended Data Fig. 1). In the case of the killing mechanism genes, expression was positively correlated with relative abundance of two bacterial taxa (out of the top 100): a member of the SUP05 clade of Gammaproteobacteria and an uncharacterized *Flavobacteriaceae* (Pearson's $r = 0.53$, $P < 0.05$, d.f. = 12). Antagonistic genes encoded type I secretion and efflux systems for toxins and antibiotics, whereas resistance genes encoded antibiotic resistance and detoxification. Whether such gene products result in positive or negative interactions is unclear, for example, toxin and polyketide export can provide defence for associated organisms[37,38].

Positive biotic interaction dimensions were suggested by variable expression for synthesis or utilization of three cofactors and six B vitamins through the bloom stages. *R. pomeroyi* had elevated transcription of genes linked to pyrroloquinoline quinone (coenzyme PQQ) in the peak-bloom invasions and thiamine, nicotinamide, vitamin B_3, riboflavin, pyridoxal phosphate, pantothenate, biotin, molybdopterin and folate in the late invasions (Fig. 3). The B vitamins cannot be synthesized by many marine phytoplankton and yet are required for key enzymatic reactions, a deficit that can be relieved by bacterial release[39,40]. The vitamin responses by *R. pomeroyi* may reflect shifts in exogenous availability of these molecules or their precursors, or biotic interactions that affect the bacterium's synthesis rates.

Differences in transcription of motility-related genes suggested a patchy distribution of deterrents or resources during the bloom. *R. pomeroyi* made the greatest investment in building motility machinery when invading the bloom peak, and less as it aged. The bacterium also invested in pilus assembly genes, for attachment or conjugation, and quorum-sensing genes, for cell-to-cell chemical signalling, with increased importance of both in peak-bloom invasions. *R. pomeroyi* harbours a gene transfer agent system[34] that packages random ~5-kb genome fragments into virus-like particles released extracellularly to initiate intraspecific gene transfer[41]. Transcription of the gene transfer agent was invoked on six consecutive invasions in mid-October, suggesting a persistent environmental condition triggering initiation of DNA transfer. Expression of this system highlights a mechanism by which niche dimensions could evolve over relatively few generations[42,43], particularly for bacteria that have specific genetic mechanisms that enhance rates of horizontal gene transfer[44].

Stress niche dimensions. On both peak- and late-bloom dates, *R. pomeroyi* encountered environmental conditions eliciting enhanced transcription of genes for repair and recombination of DNA, refolding damaged proteins[45] and responding to oxidative stress (Fig. 3 and Supplementary Table 2). The *R. pomeroyi* genome contains two σ-32 genes that were invoked on introduction into the late-bloom environment and may be master regulators of stress responses[45–47]. Light exposure and temperature were at ambient laboratory conditions (with incubation temperature differing by 4–7 °C from in situ) for all invasion experiments, and salinity differences between samples were minor (33.4–33.6 PSU); these factors were therefore not likely to have differentially affected bacterial viability. Influence from exposure to reactive oxygen species, formed from either dissolved organic matter or the microbial community[48,49], is a potential driver of these responses.

Niche boundaries. The sequential invasion experiments characterized features of a coastal phytoplankton bloom eliciting responses from a bacterium, but not whether the values of those features allowed its survival and reproduction; thus transcriptomic data addressed niche dimensions but not niche space. We looked for attributes of *R. pomeroyi*'s transcriptome that indicate when the bacterium would have succeeded in the 'growth and spread' stage[21] had the invasion been carried to completion. Transcription of ribosomal proteins was maximum in late-bloom invasions (Fig. 4a), accounting for a twofold greater share of the transcript pool in late versus peak experiments (2.3% versus 1.2% for the two final versus two initial experiments; Mann–Whitney *U*-test, $P < 0.01$, two tailed). As up to 40% of a bacterium's energy is allocated to protein synthesis, cells strictly regulate ribosomal protein transcripts to match available resources[50–52]; experimental studies have confirmed that this is the case for *R. pomeroyi*[19,53]. The bacterium's transcription of σ-70, the major regulator of housekeeping gene expression during growth[54], was also maximum in late-bloom invasions, accounting for a more than fourfold greater share of the transcriptome in late versus peak experiments (0.83% versus 0.20%; Mann–Whitney *U*-test, $P < 0.01$, two tailed) (Fig. 4a). Experimental studies have similarly confirmed that the *R.*

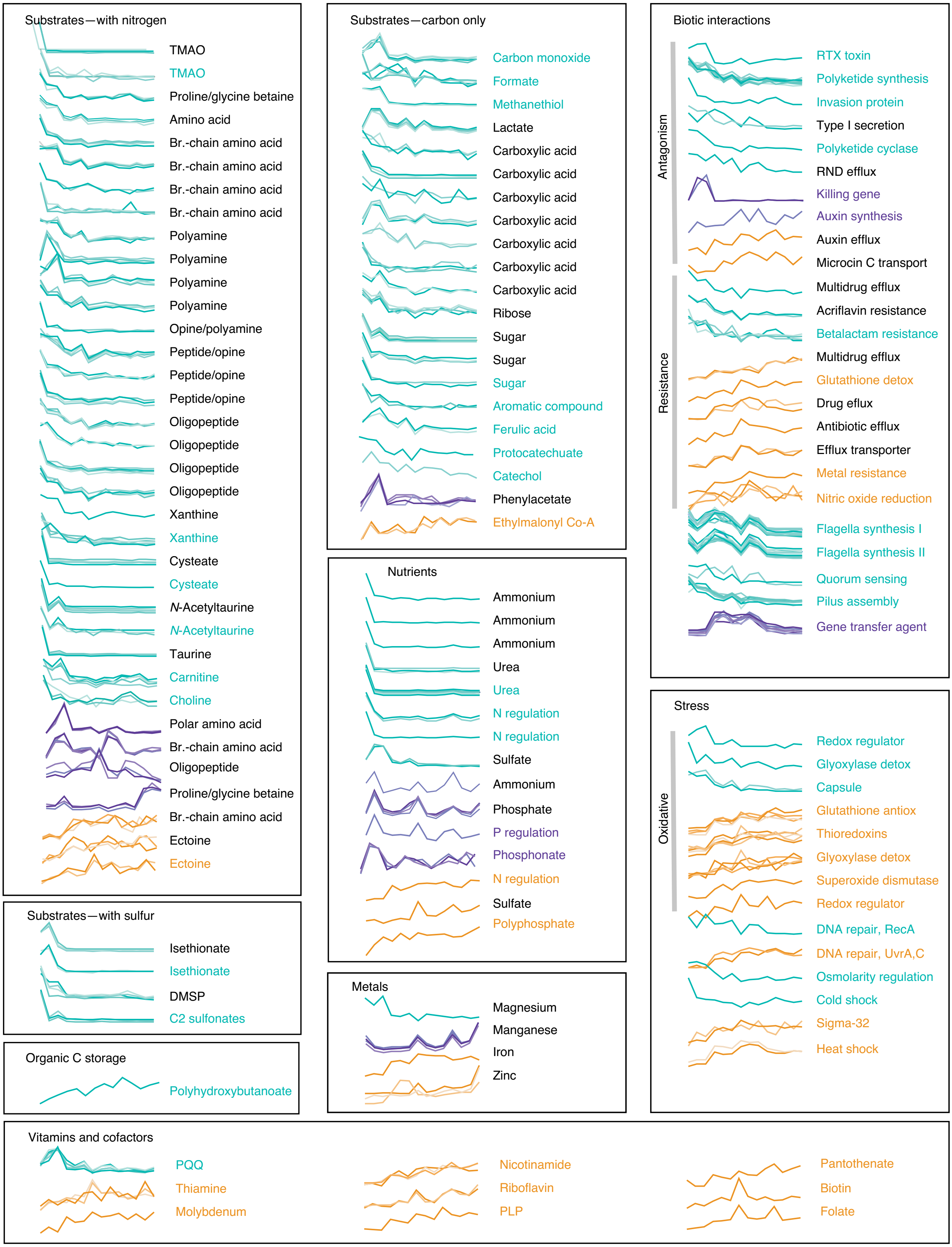

Fig. 3 | Time course of relative gene expression indicating *R. pomeroyi*'s responses to niche dimensions. Functional assignments in black denote transporters. Genes are organized by dimension type and coloured by expression module: peak-bloom supermodule, turquoise lines; late-bloom supermodule, orange lines; other modules, purple lines. Multiple lines represent protein subunits or functionally related genes. Br., branched. All genes shown are significantly different at the two highest and lowest time points based on two-sided DeSeq2 analysis (adjusted $P \leq 0.05$ with Benjamini–Hochberg correction). Data are mean *z*-scores ($n = 3$ except for 30 September (second data point from the left) where $n = 2$). PLP, Pyridoxal phosphate; Uvr, ultraviolet radiation.

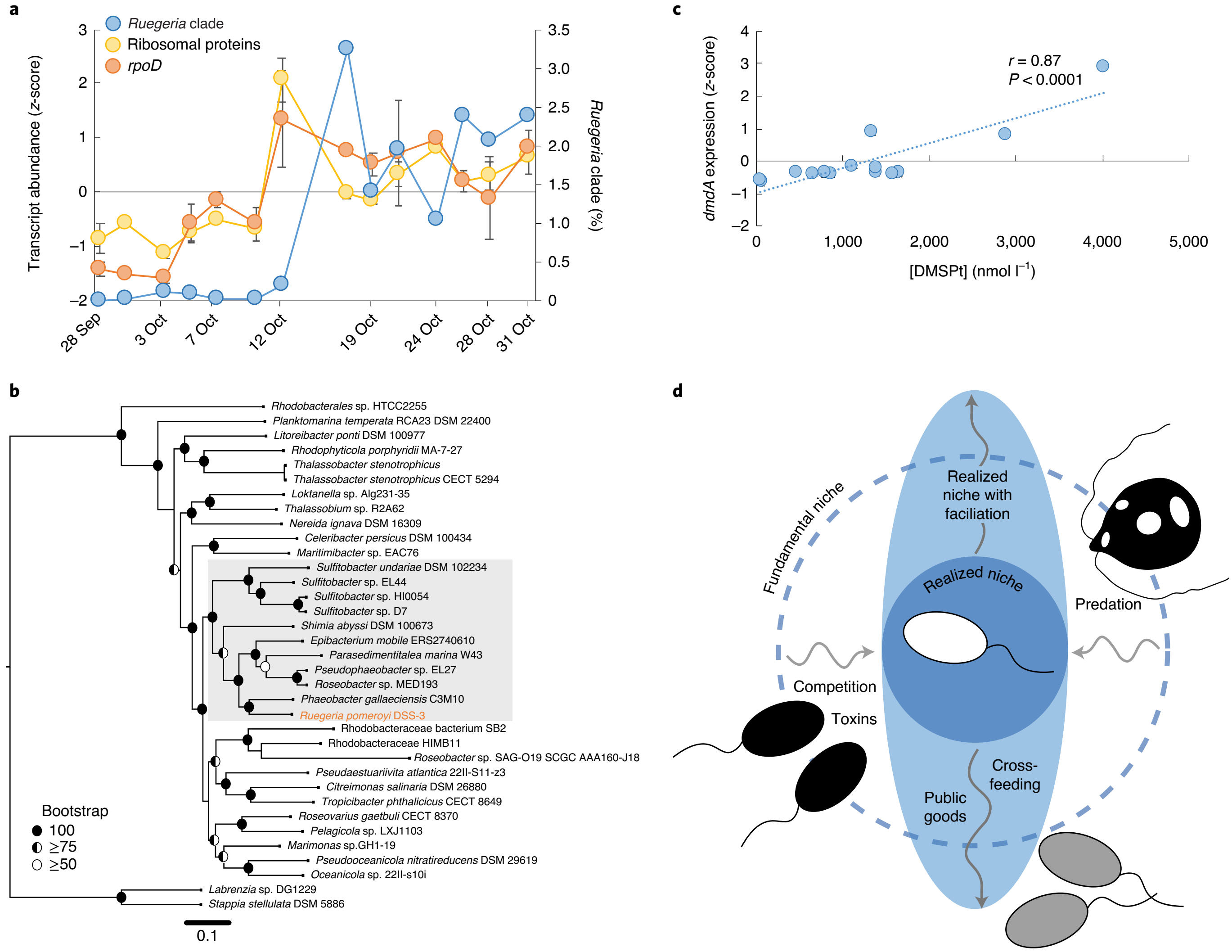

Fig. 4 | Characterization of *R. pomeroyi* niche boundaries. **a**, Growth metrics of *R. pomeroyi* on 14 dates during the Monterey Bay bloom in the autumn of 2016. Expression of 54 ribosomal protein genes and *rpoD* (σ-70 factor) (left axis) are plotted as a *z*-score normalization of mean values ($n=3\pm1$ s.d., except for 30 September where $n=2$). *Ruegeria* clade abundance in the bloom communities without added *R. pomeroyi* (right axis) is shown as a percentage of Rhodobacteraceae sequences ($n=2$ or 3). **b**, Phylogenomic tree of genomes most closely related to Rhodobacteraceae ASVs in 16S rRNA gene libraries (Extended Data Fig. 1); grey shading indicates the *Ruegeria* clade shown in **a**. The scale bar represents the number of substitutions per site. **c**, Correlation of DMSP concentrations with relative expression of DMSP catabolism gene *dmdA* in invading *R. pomeroyi* ($n=3$ except for 30 September where $n=2$). **d**, Conceptualization of a microbial fundamental niche (dashed line) reflecting the environmental conditions determining where net growth rate is >0 in the absence of biotic interactions. Negative biotic interactions such as competition and toxins narrow niche space to the realized niche (dark-blue circle), whereas positive biotic interactions, such as the provision of resources, can expand the realized niche space beyond the fundamental niche along certain dimensions. Modified from ref. [74].

pomeroyi rpoD transcript inventory correlates with growth rate[53]. A third growth proxy was based on abundance in the pre-invasion community 16S rRNA gene pool of the Rhodobacteraceae subclade to which *R. pomeroyi* belongs (Fig. 4b), an index independent of transcription patterns. This revealed that late-bloom conditions supported >100-fold higher *Ruegeria* clade populations compared with peak bloom (Fig. 4a) (2.22% versus 0.02% of Rhodobacteraceae 16S rRNA sequences; Mann–Whitney *U*-test, $P<0.05$, two tailed). Yet agreement among these three indices that growth potential was actually higher for invading *R. pomeroyi* during the late bloom is counter to indications from transporter expression that substrates supporting the bacterium's growth were maximally available at the peak bloom (Fig. 3).

One explanation for asynchrony between the opportunity for substrate acquisition and the ability to grow, signalling a narrowing of the niche, is that the bacterium's transport/catabolism transcripts are unreliable reporters of substrate availability because they do not track closely with substrate supply. Countering this, measures of the concentration of the substrate DMSP at each invasion date[22] were strongly correlated with relative expression levels of the DMSP catabolism gene *dmdA* in invading *R. pomeroyi* (Pearson's $r=0.87$, $P<0.0001$, d.f. = 12) (Fig. 4c). Thus, for a key substrate in the *Akashiwo* bloom[55], gene expression patterns were synchronized with substrate supply, agreeing with previous demonstrations of substrate-induced transporter expression in this bacterium[14,56–60]. Alternatively, the bacterium may have been limited by inorganic nitrogen availability at the peak of the bloom and unable to capitalize on substrate supply. Transcription patterns suggest that a variety of alternative organic nitrogen molecules was being targeted for uptake during the peak bloom (Fig. 3).

A third possible explanation for the mismatch in timing of substrate transporter expression and growth is that *R. pomeroyi*'s ability to capitalize on substrate availability was inhibited by negative biotic interactions at the bloom peak. Secondary metabolite release by the red tide species *A. sanguinea* is linked to toxicity in seabirds, fish and invertebrates[61–63], and potentially narrowed the realized niche space of *R. pomeroyi*. Measures of native bacterial community uptake of DMSP were unusually low on peak-bloom dates, with turnover of dissolved DMSP averaging 10% per day compared with typical bloom values of 30–100% per day[22,64,65]. The native bacterial community therefore processed DMSP from bloom seawater at low rates despite high availability, and *R. pomeroyi* may have been similarly affected. Thus, despite the presence of growth-supporting substrates recognized by transporter-binding proteins (a permissive condition in one realized niche dimension of the bacterium), inhibitory metabolites may have depressed its growth (a constraining condition in another dimension). Expression of bacterial genes for the synthesis of an RTX toxin, a secreted protein with cytotoxic and haemolytic activities towards eukaryotic cells[66], and two polyketides was also highest at the peak bloom. An indication that biotic dimensions imposed by co-occurring microbes can be as important as resource dimensions supporting growth in the niche space of phytoplankton-associated bacteria was unexpected, because resource-driven assembly of bacterial communities is common in coastal phytoplankton blooms[67–71]. Recognition of the importance of non-trophic biotic interactions in determining surface ocean microbial viability is increasing[72,73].

Discussion

The mRNA pools of a marine bacterium introduced into an ongoing coastal phytoplankton bloom in a standardized physiological state served as a proxy for the environmental factors making up its niche dimensions. Transcriptional responses by *R. pomeroyi*, including regulating substrate and nutrient uptake and invoking hormone and antimicrobial production, identified chemical and biotic features of the environment, both positive and negative, that affected viability.

Negative biotic interactions are included in classic niche theory as features that narrow an organism's niche from fundamental to realized, for example, by competition for resources or toxicity from secondary metabolites[8,27] (Fig. 4d). The inclusion in niche theory of positive biotic interactions (that is, 'facilitation'[74]) such as public goods dimensions (for example, vitamins[75]) or mutualism dimensions (for example, cross-feeding[75,76]) implies that, absent from early formulations, the realized niche can extend beyond the fundamental niche when interacting species broaden conditions under which a microbe can survive[27,74] (Fig. 4d). This perspective is not necessarily counter to Hutchinson's conceptualizations[27], and can be reconciled if the Hutchinsonian fundamental niche concept is defined to include positive biotic interactions, whereas the realized niche concept includes only negative ones. It is an aspect of niche theory that may be particularly important in highly interconnected microbial communities such as coastal blooms.

The niche dimensions determining a species' success in natural environments are notoriously difficult to identify. This is because there are a vast number of environmental features to consider, many of which are not yet recognized[77], and because correlated signals between inventoried features and microbial responses do not resolve causal relationships. Ecological invasion studies, in their simplest form, add taxa to extant natural communities to uncover principles governing the ability of invading species to successfully exploit the invaded community's resources[20]. We leveraged this approach to capture niche dimensions experimentally by introducing a metabolically responsive species representative of marine bacteria with life history strategies linked to phytoplankton-derived metabolites[26,78] into an environment that it might reasonably invade. Each experimental invasion reported the species' de novo detection of environmental conditions, with transcriptional responses spotlighting multiple substrates and non-trophic biotic interactions that influenced ecological success in a dinoflagellate-dominated phytoplankton bloom. Invasion experiments with well-studied microorganisms can bridge the gap between ecologically relevant field studies and mechanistically informative model organism studies, thereby improving understanding of the factors that determine where bacterial species survive and function in the seawater environment.

Methods

Experimental setup. The pre-incubation protocol for *R. pomeroyi* DSS-3 began 2 d before each invasion experiment. The bacterium was inoculated into ½ YTSS liquid medium and grown overnight to exponential phase at 30 °C. Cells were then washed twice, inoculated into marine basal medium (MBM)[79] with 10 mM glucose, and incubated at 30 °C for ~26 h. After washing three times and resuspending in artificial seawater (28 g l^{-1}; Sigma sea salts), the bacterium was added into triplicate 350-ml aliquots of unfiltered Monterey Bay surface seawater collected at Station M0 (ref. [80]) at approximately 10:00 Pacific Standard Time, which achieved a ratio of ~1:1 *R. pomeroyi* cells:native bacteria. Incubations were stirred at 120 rev min^{-1} at ambient temperature (24 °C) and light for 90 min and then filtered sequentially through 2-μm polycarbonate filters to remove most non-bacterial community members and 0.2-μm polycarbonate filters to collect the bacterial size fraction. Filters were flash frozen in liquid nitrogen. Two control experiments were set up in which *R. pomeroyi* cells were prepared, as described above, for the field studies, but inoculated into defined media consisting of MBM with either no substrate or 10 mM glucose (Fig. 1b).

RNA extraction and sequencing. RNA was extracted from filters using the ZymoBIOMICS RNA Miniprep Kit (Zymo Research), treated with Turbo DNase (Invitrogen) and cleaned using RNA Clean & Concentrator (Zymo Research). Ribosomal RNA was removed using the Ribo-Zero Bacteria Kit (Illumina). Stranded RNA-sequencing libraries were prepared and sequenced using an Illumina Next-Seq SE75 High Output flow cell at the Georgia Genomics and Bioinformatics Core (University of Georgia).

Bioinformatic analysis. The FASTX toolkit was used to retain reads with a minimum quality score of 20 over 80% of read length. Reads were mapped to the *R. pomeroyi* genome using BWA[81] and counted using HTSeq[82]. Genes with zero reads mapping in more than 10% of samples were removed from further analysis. Counts were converted to transcripts per million. Weighted transcriptomic correlation network analysis was performed on *z*-score-transformed transcripts per million to cluster genes based on their expression across sample dates into modules within a correlation network, using the blockwiseModules function from the R package WGCNA with parameters power = 16, minModuleSize = 20 and networkType = 'signed'[83]. Differential expression of genes between sample dates was calculated using DESeq2 (ref. [84]). PCA was carried out on mean-normalized transcripts per million using the R program prcomp.

Environmental data. Bacteria were counted by flow cytometry, and eukaryotic microbes and cyanobacteria by epifluorescence microscopy[80]. Cells were assigned to taxonomic groups during epifluorescence counting, and carbon content was calculated for eukaryotic and cyanobacterial taxa based on cell size, shape and volume. Total particulate + dissolved DMSP concentrations and bacterial uptake rates were measured in triplicate at each sample date[22]. The 16S and 18S rRNA gene libraries were analysed from seawater collected from Station M0 at the time of each *R. pomeroyi* addition as described previously[80]. The SILVA v.132 rRNA gene database (16S)[85] and the Protist Ribosomal Reference database (PR2; 18S)[86] were used to classify sequences. Heterotrophic protist amplicon sequence variants (ASVs) were removed before community analysis. UPGMA clustering of unweighted UniFrac distances was run in Qiime2 (ref. [87]).

***Ruegeria* clade abundance.** The 16S rRNA gene ASVs from the pre-invasion 16S rRNA gene libraries classified as Rhodobacteraceae were aligned using blastn to the Joint Genome Institute IMG/M All Isolates database. Top hits to a marine Rhodobacteraceae genome were used to construct a phylogenomic tree using GToTree v.1.4.1 (ref. [88]) based on hidden Markov model profiles of 117 alphaproteobacterial single-copy genes. ASV counts were mapped on to the tree, and relative abundance of a well-supported clade that included the *R. pomeroyi* genome was calculated as a percentage of all Rhodobacteraceae ASV hits.

Reporting Summary. Further information on research design is available in the Nature Research Reporting Summary linked to this article.

Data availability

Data that support the findings of the present study have been deposited in the National Center for Biotechnology Information's Sequence Read Archive with BioProject nos. PRJNA641119 (RNA-seq) and PRJNA511156–PRJNA511331

(16S and 18S rRNA data), and the Biological and Chemical Oceanography Data Management Office under https://doi.org/10.1575/1912/bco-dmo.756413.2 at https://www.bco-dmo.org/dataset/756413/data (environmental data). Source data are provided with this paper.

Received: 9 June 2020; Accepted: 11 December 2020;
Published online: 25 January 2021

References

1. Carlson, C. A. et al. Seasonal dynamics of SAR11 populations in the euphotic and mesopelagic zones of the northwestern Sargasso Sea. *ISME J.* **3**, 283–295 (2009).
2. Palovaara, J. et al. Stimulation of growth by proteorhodopsin phototrophy involves regulation of central metabolic pathways in marine planktonic bacteria. *Proc. Natl Acad. Sci. USA* **111**, E3650–E3658 (2014).
3. Poretsky, R. S., Sun, S., Mou, X. & Moran, M. A. Transporter genes expressed by coastal bacterioplankton in response to dissolved organic carbon. *Environ. Microbiol.* **12**, 616–627 (2010).
4. Church, M. J., Hutchins, D. A. & Ducklow, H. W. Limitation of bacterial growth by dissolved organic matter and iron in the Southern Ocean. *Appl. Environ. Microbiol.* **66**, 455–466 (2000).
5. Persson, O. P. et al. High abundance of virulence gene homologues in marine bacteria. *Environ. Microbiol.* **11**, 1348–1357 (2009).
6. Yeung, L. Y. et al. Impact of diatom–diazotroph associations on carbon export in the Amazon River plume. *Geophys. Res. Lett.* **39**, L18609 (2012).
7. Colwell, R. K. & Fuentes, E. R. Experimental studies of the niche. *Annu. Rev. Ecol. Syst.* **6**, 281–310 (1975).
8. Hutchinson, G. E. Concluding remarks. *Cold Spring Harb. Symp. Quant. Biol.* **22**, 415–427 (1957).
9. Cohan, F. M. What are bacterial species? *Annu. Rev. Microbiol.* **56**, 457–487 (2002).
10. Erguder, T. H., Boon, N., Wittebolle, L., Marzorati, M. & Verstraete, W. Environmental factors shaping the ecological niches of ammonia-oxidizing archaea. *FEMS Microbiol. Rev.* **33**, 855–869 (2009).
11. Meier, D. V. et al. Niche partitioning of diverse sulfur-oxidizing bacteria at hydrothermal vents. *ISME J.* **11**, 1545–1558 (2017).
12. Martens-Habbena, W., Berube, P. M., Urakawa, H., José, R. & Stahl, D. A. Ammonia oxidation kinetics determine niche separation of nitrifying Archaea and Bacteria. *Nature* **461**, 976–979 (2009).
13. Gifford, S. M., Sharma, S., Booth, M. & Moran, M. A. Expression patterns reveal niche diversification in a marine microbial assemblage. *ISME J.* **7**, 281–298 (2013).
14. Landa, M., Burns, A. S., Roth, S. J. & Moran, M. A. Bacterial transcriptome remodeling during sequential co-culture with a marine dinoflagellate and diatom. *ISME J.* **11**, 2677–2690 (2017).
15. Ottesen, E. A. et al. Pattern and synchrony of gene expression among sympatric marine microbial populations. *Proc. Natl Acad. Sci. USA* **110**, E488–E497 (2013).
16. Galambos, D., Anderson, R. E., Reveillaud, J. & Huber, J. A. Genome-resolved metagenomics and metatranscriptomics reveal niche differentiation in functionally redundant microbial communities at deep-sea hydrothermal vents. *Environ. Microbiol.* **21**, 4395–4410 (2019).
17. Nuccio, E. E. et al. Niche differentiation is spatially and temporally regulated in the rhizosphere. *ISME J.* **14**, 999–1014 (2020).
18. Shaiber, A. & Eren, A. M. Composite metagenome-assembled genomes reduce the quality of public genome repositories. *mBio* **10**, e00725-19 (2019).
19. Cottrell, M. T. & Kirchman, D. L. Transcriptional control in marine copiotrophic and oligotrophic bacteria with streamlined genomes. *Appl. Environ. Microbiol.* **82**, 6010–6018 (2016).
20. Bell, T. Next-generation experiments linking community structure and ecosystem functioning. *Environ. Microbiol. Rep.* **11**, 20–22 (2019).
21. Mallon, C. A., Van Elsas, J. D. & Salles, J. F. Microbial invasions: the process, patterns, and mechanisms. *Trends Microbiol.* **23**, 719–729 (2015).
22. Kiene, R. P. et al. Unprecedented DMSP concentrations in a massive dinoflagellate bloom in Monterey Bay, CA. *Geophys. Res. Lett.* **46**, 12279–12288 (2019).
23. Anderson, S. R., Diou-Cass, Q. P. & Harvey, E. L. Short-term estimates of phytoplankton growth and mortality in a tidal estuary. *Limnol. Oceanogr.* **63**, 2411–2422 (2018).
24. Anderson, S. R. & Harvey, E. L. Seasonal variability and drivers of microzooplankton grazing and phytoplankton growth in a subtropical estuary. *Front Mar. Sci.* **6**, 174–174 (2019).
25. González, J. M. et al. *Silicibacter pomeroyi* sp. nov. and *Roseovarius nubinhibens* sp. nov., dimethylsulfoniopropionate-demethylating bacteria from marine environments. *Int. J. Syst. Evol. Microbiol.* **53**, 1261–1269 (2003).
26. Luo, H. & Moran, M. A. Evolutionary ecology of the marine Roseobacter clade. *Microbiol. Mol. Biol. Rev.* **78**, 573–587 (2014).
27. Colwell, R. K. & Rangel, T. F. Hutchinson's duality: the once and future niche. *Proc. Natl Acad. Sci. USA* **106**, 19651–19658 (2009).
28. Holt, R. D. Bringing the Hutchinsonian niche into the 21st century: ecological and evolutionary perspectives. *Proc. Natl Acad. Sci. USA* **106**, 19659–19665 (2009).
29. Alneberg, J. et al. Ecosystem-wide metagenomic binning enables prediction of ecological niches from genomes. *Commun. Biol.* **3**, 119 (2020).
30. Baltar, F. et al. Towards integrating evolution, metabolism, and climate change studies of marine ecosystems. *Trends Ecol. Evol.* **34**, 1022–1033 (2019).
31. Muller, E. E. Determining microbial niche breadth in the environment for better ecosystem fate predictions. *mSystems* **4**, e00080-19 (2019).
32. Chan, L.-K. et al. Transcriptional changes underlying elemental stoichiometry shifts in a marine heterotrophic bacterium. *Front. Microbiol.* **3**, 159 (2012).
33. Kudela, R. M., Seeyave, S. & Cochlan, W. P. The role of nutrients in regulation and promotion of harmful algal blooms in upwelling systems. *Prog. Oceanogr.* **85**, 122–135 (2010).
34. Moran, M. A. et al. Genome sequence of *Silicibacter pomeroyi* reveals adaptations to the marine environment. *Nature* **432**, 910–913 (2004).
35. Amin, S. A. et al. Interaction and signalling between a cosmopolitan phytoplankton and associated bacteria. *Nature* **522**, 98–101 (2015).
36. Sharpe, G. C., Gifford, S. M. & Septer, A. N. A model *Roseobacter* employs a diffusible killing mechanism to eliminate competitors. *mSystems* **5**, e00443-20 (2020).
37. Gil-Turnes, M. S., Hay, M. E. & Fenical, W. Symbiotic marine bacteria chemically defend crustacean embryos from a pathogenic fungus. *Science* **246**, 116–118 (1989).
38. Lopanik, N., Lindquist, N. & Targett, N. Potent cytotoxins produced by a microbial symbiont protect host larvae from predation. *Oecologia* **139**, 131–139 (2004).
39. Croft, M. T., Lawrence, A. D., Raux-Deery, E., Warren, M. J. & Smith, A. G. Algae acquire vitamin B12 through a symbiotic relationship with bacteria. *Nature* **438**, 90–93 (2005).
40. Sañudo-Wilhelmy, S. A., Gómez-Consarnau, L., Suffridge, C. & Webb, E. A. The role of B vitamins in marine biogeochemistry. *Annu. Rev. Mar. Sci.* **6**, 339–367 (2014).
41. Biers, E. J. et al. Occurrence and expression of gene transfer agent genes in marine bacterioplankton. *Appl. Environ. Microbiol.* **74**, 2933–2939 (2008).
42. Gravel, D. et al. Experimental niche evolution alters the strength of the diversity–productivity relationship. *Nature* **469**, 89–94 (2011).
43. Vergin, K. L. et al. High intraspecific recombination rate in a native population of *Candidatus* Pelagibacter ubique (SAR11). *Environ. Microbiol.* **9**, 2430–2440 (2007).
44. McDaniel, L. D. et al. High frequency of horizontal gene transfer in the oceans. *Science* **330**, 50–50 (2010).
45. Nuss, A. M., Glaeser, J., Berghoff, B. A. & Klug, G. Overlapping alternative sigma factor regulons in the response to singlet oxygen in *Rhodobacter sphaeroides*. *J. Bacteriol.* **192**, 2613–2623 (2010).
46. Berghoff, B. A. et al. Anoxygenic photosynthesis and photooxidative stress: a particular challenge for Roseobacter. *Environ. Microbiol.* **13**, 775–791 (2011).
47. Zhao, K., Liu, M. & Burgess, R. R. The global transcriptional response of *Escherichia coli* to induced σ32 protein involves σ32 regulon activation followed by inactivation and degradation of σ32 in vivo. *J. Biol. Chem.* **280**, 17758–17768 (2005).
48. Diaz, J. M. et al. Widespread production of extracellular superoxide by heterotrophic bacteria. *Science* **340**, 1223–1226 (2013).
49. Wietz, M., Duncan, K., Patin, N. V. & Jensen, P. R. Antagonistic interactions mediated by marine bacteria: the role of small molecules. *J. Chem. Ecol.* **39**, 879–891 (2013).
50. Maguire, B. A. Inhibition of bacterial ribosome assembly: a suitable drug target? *Microbiol. Mol. Biol. Rev.* **73**, 22–35 (2009).
51. Wei, Y. et al. High-density microarray-mediated gene expression profiling of *Escherichia coli*. *J. Bacteriol.* **183**, 545–556 (2001).
52. Wilson, D. N. & Nierhaus, K. H. The weird and wonderful world of bacterial ribosome regulation. *Crit. Rev. Biochem. Mol. Biol.* **42**, 187–219 (2007).
53. Vinas, N. *Relationships between Growth Rate and Gene Expression in* Ruegeria pomeroyi *DSS-3, a Model Marine Alphaproteobacterium*. MSc thesis, Clemson Univ. (2015).
54. Ishihama, A. Functional modulation of *Escherichia coli* RNA polymerase. *Annu. Rev. Microbiol.* **54**, 499–518 (2000).
55. González, J. M., Kiene, R. P. & Moran, M. A. Transformation of sulfur compounds by an abundant lineage of marine bacteria in the α-subclass of the class Proteobacteria. *Appl. Environ. Microbiol.* **65**, 3810–3819 (1999).
56. Denger, K., Lehmann, S. & Cook, A. M. Molecular genetics and biochemistry of *N*-acetyltaurine degradation by *Cupriavidus necator* H16. *Microbiology* **157**, 2983–2991 (2011).
57. Lidbury, I., Murrell, J. C. & Chen, Y. Trimethylamine *N*-oxide metabolism by abundant marine heterotrophic bacteria. *Proc. Natl Acad. Sci. USA* **111**, 2710–2715 (2014).

58. Mou, X., Sun, S., Edwards, R. A., Hodson, R. E. & Moran, M. A. Bacterial carbon processing by generalist species in the coastal ocean. *Nature* **451**, 708–711 (2008).
59. Schulz, A. et al. Feeding on compatible solutes: a substrate-induced pathway for uptake and catabolism of ectoines and its genetic control by EnuR. *Environ. Microbiol.* **19**, 926–946 (2017).
60. Weinitschke, S., Sharma, P. I., Stingl, U., Cook, A. M. & Smits, T. H. Gene clusters involved in isethionate degradation by terrestrial and marine bacteria. *Appl. Environ. Microbiol.* **76**, 618–621 (2010).
61. Jessup, D. A., Miller, M. A., Ryan, J. P., Nevins, H. M. & Kerkering, H. A. Mass stranding of marine birds caused by a surfactant-producing red tide. *PLoS ONE* **4**, 4550 (2009).
62. Jones, T. et al. Mass mortality of marine birds in the Northeast Pacific caused by *Akashiwo sanguinea*. *Mar. Ecol. Prog. Ser.* **579**, 111–127 (2017).
63. Xu, N. et al. Acute toxicity of the cosmopolitan bloom-forming dinoflagellate *Akashiwo sanguinea* to finfish, shellfish, and zooplankton. *Aquat. Microb. Ecol.* **80**, 209–222 (2017).
64. Kiene, R. P. & Linn, L. J. Distribution and turnover of dissolved DMSP and its relationship with bacterial production and dimethylsulfide in the Gulf of Mexico. *Limnol. Oceanogr.* **45**, 849–861 (2000).
65. Motard-Côté, J., Kieber, D. J., Rellinger, A. & Kiene, R. P. Influence of the Mississippi River plume and non-bioavailable DMSP on dissolved DMSP turnover in the northern Gulf of Mexico. *Environ. Chem.* **13**, 280–280 (2016).
66. Lally, E. T., Hill, R. B., Kieba, I. R. & Korostoff, J. The interaction between RTX toxins and target cells. *Trends Microbiol.* **7**, 356–361 (1999).
67. Billen, G. & Fontigny, A. Dynamics of a *Phaeocystis*-dominated spring bloom in Belgian coastal waters. II. Bacterioplankton dynamics. *Mar. Ecol. Prog. Ser.* **37**, 249–257 (1987).
68. Buchan, A., LeCleir, G. R., Gulvik, C. A. & González, J. M. Master recyclers: features and functions of bacteria associated with phytoplankton blooms. *Nat. Rev. Microbiol.* **12**, 686–698 (2014).
69. Bunse, C. et al. Spatio-temporal interdependence of bacteria and phytoplankton during a Baltic Sea spring bloom. *Front. Microbiol.* **7**, 517–517 (2016).
70. Pinhassi, J. et al. Changes in bacterioplankton composition under different phytoplankton regimens. *Appl. Environ. Microbiol.* **70**, 6753–6766 (2004).
71. Teeling, H. et al. Substrate-controlled succession of marine bacterioplankton populations induced by a phytoplankton bloom. *Science* **336**, 608–611 (2012).
72. Morris, J. J., Johnson, Z. I., Szul, M. J., Keller, M. & Zinser, E. R. Dependence of the cyanobacterium *Prochlorococcus* on hydrogen peroxide scavenging microbes for growth at the ocean's surface. *PLoS ONE* **6**, e16805 (2011).
73. Stock, F. et al. N-acyl homoserine lactone derived tetramic acids impair photosynthesis in *Phaeodactylum tricornutum*. *ACS Chem. Biol.* **14**, 198–203 (2019).
74. Bruno, J. F., Stachowicz, J. J. & Bertness, M. D. Inclusion of facilitation into ecological theory. *Trends Ecol. Evol.* **18**, 119–125 (2003).
75. Morris, J. J., Lenski, R. E. & Zinser, E. R. The black queen hypothesis: evolution of dependencies through adaptive gene loss. *mBio* **3**, e00036-12 (2012).
76. Pacheco, A. R., Moel, M. & Segrè, D. Costless metabolic secretions as drivers of interspecies interactions in microbial ecosystems. *Nat. Commun.* **10**, 103 (2019).
77. Saupe, E. E. et al. Reconstructing ecological niche evolution when niches are incompletely characterized. *Syst. Biol.* **67**, 428–438 (2018).
78. Fu, H., Uchimiya, M., Gore, J. & Moran, M. A. Ecological drivers of bacterial community assembly in synthetic phycospheres. *Proc. Natl Acad. Sci. USA* **117**, 3656–3662 (2020).
79. González, J. M., Mayer, F., Moran, M. A., Hodson, R. E. & Whitman, W. B. *Microbulbifer hydrolyticus* gen. nov., sp. nov., and *Marinobacterium georgiense* gen. nov., sp. nov., two marine bacteria from a lignin-rich pulp mill waste enrichment community. *Int. J. Syst. Evol. Microbiol.* **47**, 369–376 (1997).
80. Nowinski, B. et al. Microbial metagenomes and metatranscriptomes during a coastal phytoplankton bloom. *Sci. Data* **6**, 129 (2019).
81. Li, H. & Durbin, R. Fast and accurate short read alignment with Burrows–Wheeler transform. *Bioinformatics* **25**, 1754–1760 (2009).
82. Anders, S., Pyl, P. T. & Huber, W. Genome analysis HTSeq—a Python framework to work with high-throughput sequencing data. *Bioinformatics* **31**, 166–169 (2015).
83. Langfelder, P. & Horvath, S. WGCNA: an R package for weighted correlation network analysis. *BMC Bioinform.* **9**, 559 (2008).
84. Love, M. I., Huber, W. & Anders, S. Moderated estimation of fold change and dispersion for RNA-seq data with DESeq2. *Genome Biol.* **15**, 550–550 (2014).
85. Quast, C. et al. The SILVA ribosomal RNA gene database project: improved data processing and web-based tools. *Nucleic Acids Res.* **41**, D590–D596 (2012).
86. Guillou, L. et al. The Protist Ribosomal Reference database (PR^2): a catalog of unicellular eukaryote small sub-unit rRNA sequences with curated taxonomy. *Nucleic Acids Res.* **41**, 597–604 (2013).
87. Bolyen, E. et al. Reproducible, interactive, scalable, and extensible microbiome data science using QIIME2. *Nat. Biotechnol.* **37**, 852–857 (2019).
88. Lee, M. D. GToTree: a user-friendly workflow for phylogenomics. *Bioinformatics* **35**, 4162–4164 (2019).

Acknowledgements

We thank C. Preston, J. Birch, C. Sholin and the MBARI ESP team for providing field sampling infrastructure and expertise; S. Sharma for providing bioinformatic assistance; C. Smith, C. Thomas and K. Esson for assisting with field and laboratory techniques; R. Michisaki for providing expertise on microbial biomass estimates; and the University of Georgia Genomics and Bioinformatics Core for supplying sequencing services. This work was supported by the Simons Foundation (grant no. 542391 to M.A.M.) within the Principles of Microbial Ecosystems (PriME) Collaborative and by NSF (IOS-1656311). The rRNA amplicon sequencing was provided through the DOE Joint Genome Institute Community Sequencing Program.

Author contributions

B.N. and M.A.M. conceived of the study. B.N. collected the data. B.N. and M.A.M. analysed the data and wrote the paper.

Competing interests

The authors declare no competing interests.

Additional information

Extended data is available for this paper at https://doi.org/10.1038/s41564-020-00851-2.

Supplementary information is available for this paper at https://doi.org/10.1038/s41564-020-00851-2.

Correspondence and requests for materials should be addressed to M.A.M.

Peer review information *Nature Microbiology* thanks Virginia Armbrust and the other, anonymous, reviewer(s) for their contribution to the peer review of this work.

Reprints and permissions information is available at www.nature.com/reprints.

Publisher's note Springer Nature remains neutral with regard to jurisdictional claims in published maps and institutional affiliations.

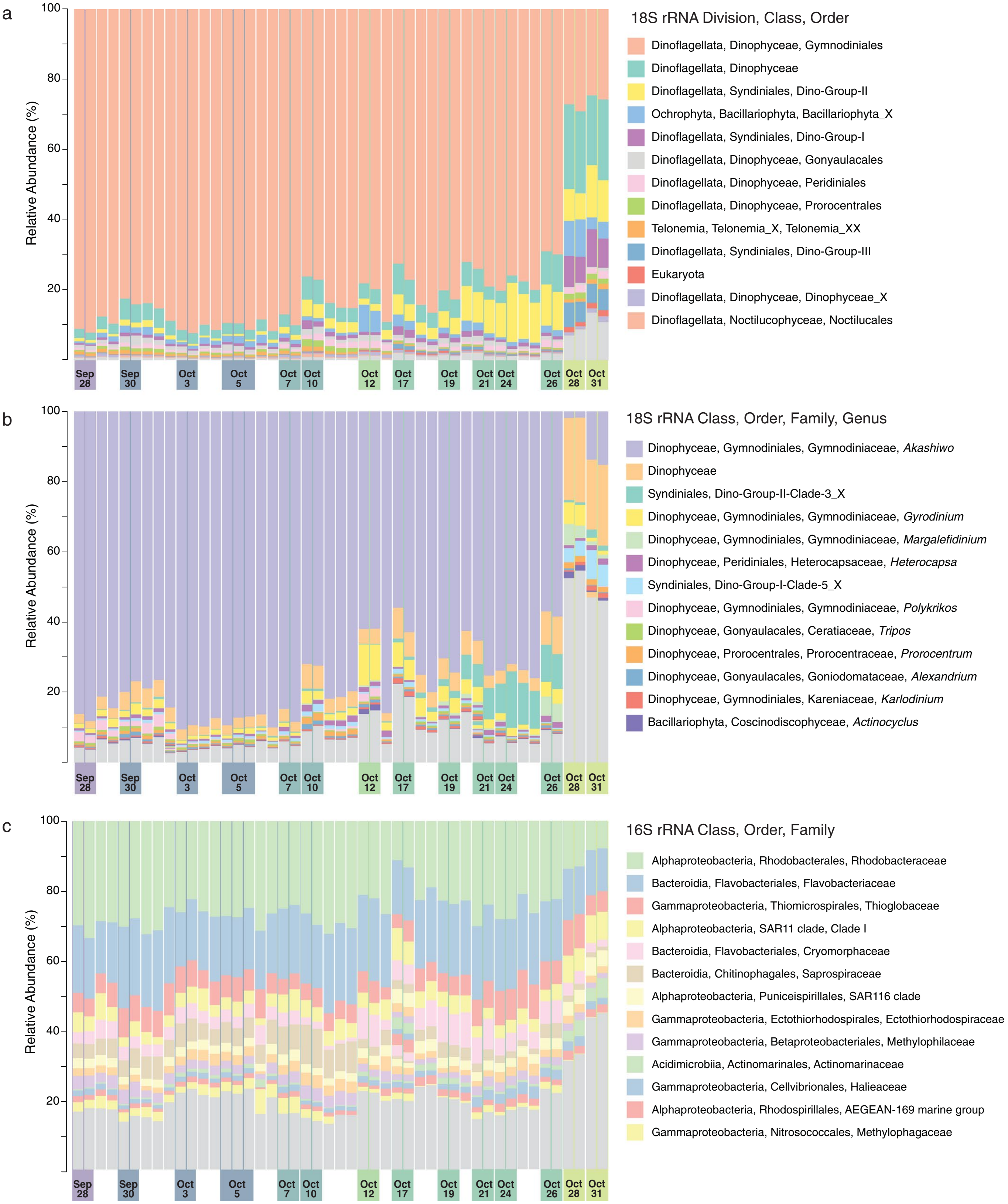

Extended Data Fig. 1 | Protist and bacterial community composition during the 2016 Monterey Bay autumn bloom based on rRNA gene sequencing. Each bar represents 1 replicate sample. **a**) 18S rRNA, order level. **b**) 18S rRNA, genus level. **c**) 16S rRNA, family level.

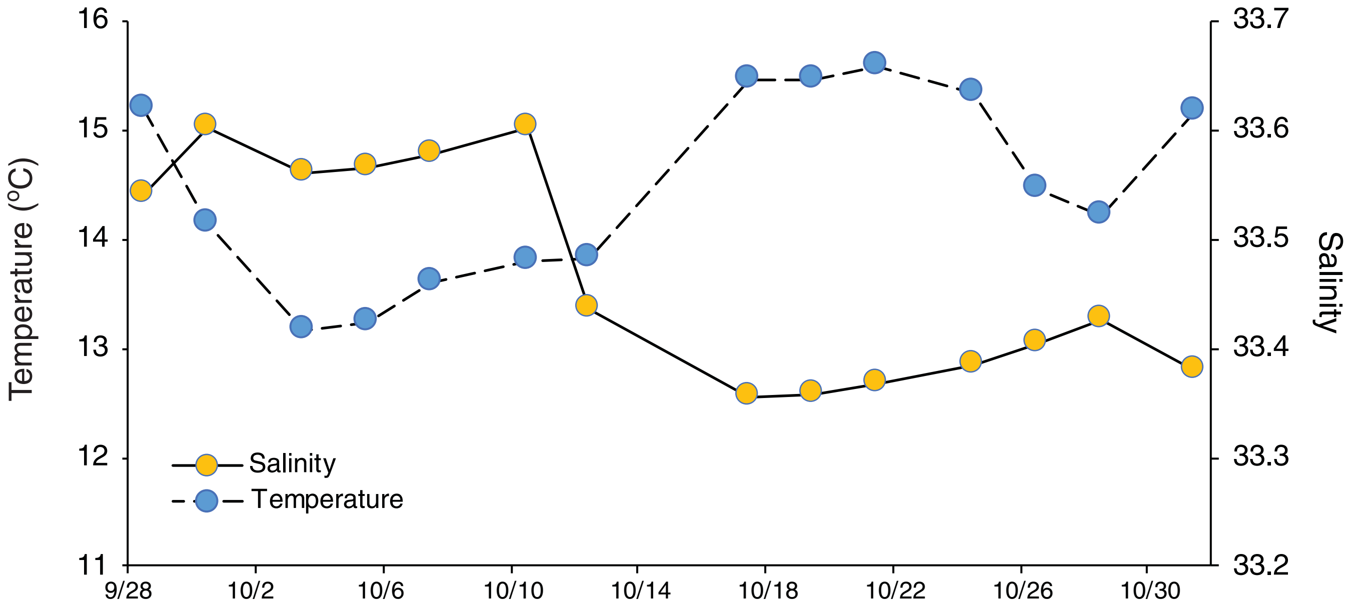

Extended Data Fig. 2 | Salinity and temperature of seawater sampled by CTD at Monterey Bay Station MO in Fall, 2016.

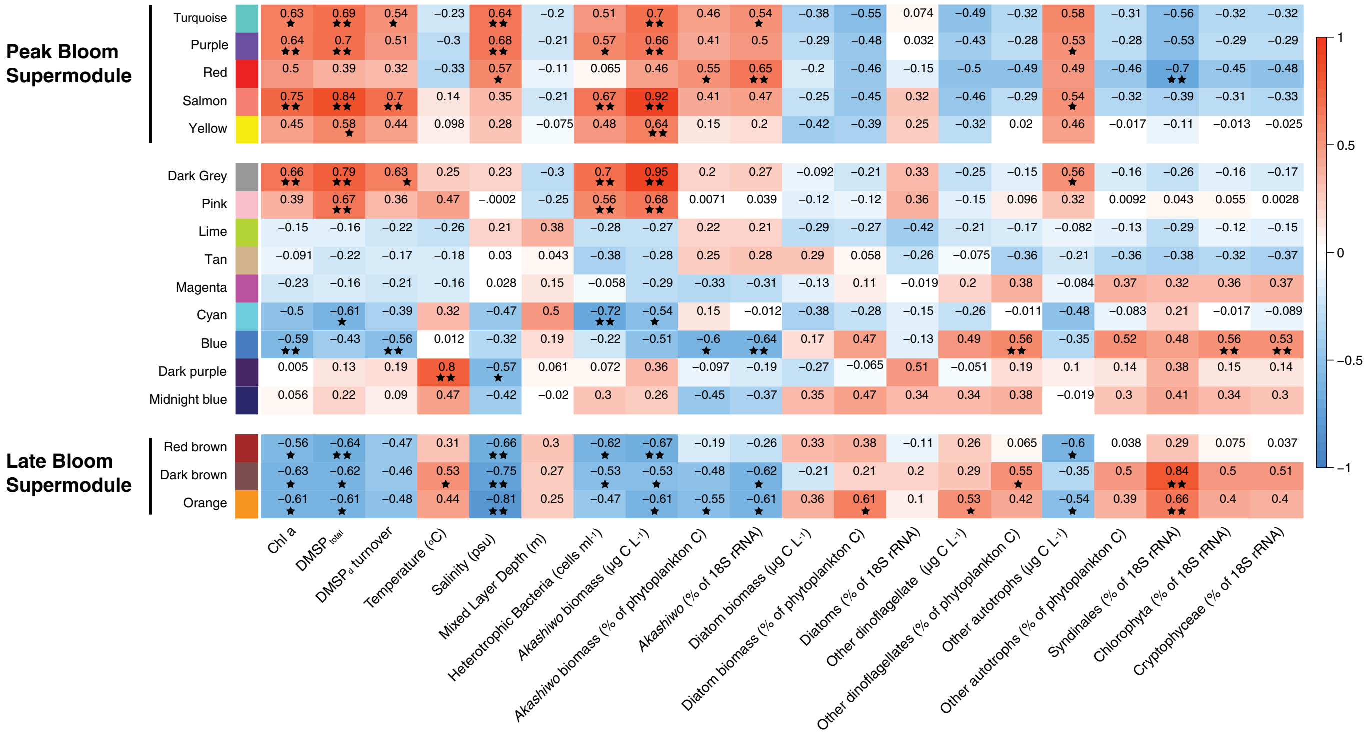

		Chl a	DMSP$_{total}$	DMSP$_d$ turnover	Temperature (°C)	Salinity (psu)	Mixed Layer Depth (m)	Heterotrophic Bacteria (cells ml^{-1})	*Akashiwo* biomass (µg C L^{-1})	*Akashiwo* biomass (% of phytoplankton C)	*Akashiwo* (% of 18S rRNA)	Diatom biomass (µg C L^{-1})	Diatom biomass (% of phytoplankton C)	Diatoms (% of 18S rRNA)	Other dinoflagellate (µg C L^{-1})	Other dinoflagellates (% of phytoplankton C)	Other autotrophs (µg C L^{-1})	Other autotrophs (% of phytoplankton C)	Syndinales (% of 18S rRNA)	Chlorophyta (% of 18S rRNA)	Cryptophyceae (% of 18S rRNA)
Peak Bloom Supermodule	Turquoise	0.63 ★	0.69 ★★	0.54 ★	−0.23	0.64 ★★	−0.2	0.51	0.7 ★★	0.46	0.54 ★	−0.38	−0.55	0.074	−0.49	−0.32	0.58	−0.31	−0.56	−0.32	−0.32
	Purple	0.64 ★★	0.7 ★★	0.51	−0.3	0.68 ★★	−0.21	0.57 ★	0.66 ★★	0.41	0.5	−0.29	−0.48	0.032	−0.43	−0.28	0.53 ★	−0.28	−0.53	−0.29	−0.29
	Red	0.5	0.39	0.32	−0.33	0.57 ★	−0.11	0.065	0.46	0.55 ★	0.65 ★★	−0.2	−0.46	−0.15	−0.5	−0.49	0.49	−0.46	−0.7 ★★	−0.45	−0.48
	Salmon	0.75 ★★	0.84 ★★	0.7 ★★	0.14	0.35	−0.21	0.67 ★★	0.92 ★★	0.41	0.47	−0.25	−0.45	0.32	−0.46	−0.29	0.54 ★	−0.32	−0.39	−0.31	−0.33
	Yellow	0.45	0.58 ★	0.44	0.098	0.28	−0.075	0.48	0.64 ★★	0.15	0.2	−0.42	−0.39	0.25	−0.32	0.02	0.46	−0.017	−0.11	−0.013	−0.025
	Dark Grey	0.66 ★★	0.79 ★★	0.63 ★	0.25	0.23	−0.3	0.7 ★★	0.95 ★★	0.2	0.27	−0.092	−0.21	0.33	−0.25	−0.15	0.56 ★	−0.16	−0.26	−0.16	−0.17
	Pink	0.39	0.67 ★★	0.36	0.47	−.0002	−0.25	0.56 ★★	0.68 ★★	0.0071	0.039	−0.12	−0.12	0.36	−0.15	0.096	0.32	0.0092	0.043	0.055	0.0028
	Lime	−0.15	−0.16	−0.22	−0.26	0.21	0.38	−0.28	−0.27	0.22	0.21	−0.29	−0.27	−0.42	−0.21	−0.17	−0.082	−0.13	−0.29	−0.12	−0.15
	Tan	−0.091	−0.22	−0.17	−0.18	0.03	0.043	−0.38	−0.28	0.25	0.28	0.29	0.058	−0.26	−0.075	−0.36	−0.21	−0.36	−0.38	−0.32	−0.37
	Magenta	−0.23	−0.16	−0.21	−0.16	0.028	0.15	−0.058	−0.29	−0.33	−0.31	−0.13	0.11	−0.019	0.2	0.38	−0.084	0.37	0.32	0.36	0.37
	Cyan	−0.5	−0.61 ★	−0.39	0.32	−0.47	0.5	−0.72 ★★	−0.54 ★	0.15	−0.012	−0.38	−0.28	−0.15	−0.26	−0.011	−0.48	−0.083	0.21	−0.017	−0.089
	Blue	−0.59 ★★	−0.43	−0.56 ★★	0.012	−0.32	0.19	−0.22	−0.51	−0.6 ★	−0.64 ★★	0.17	0.47	−0.13	0.49	0.56 ★★	−0.35	0.52	0.48	0.56 ★★	0.53 ★★
	Dark purple	0.005	0.13	0.19	0.8 ★★	−0.57 ★	0.061	0.072	0.36	−0.097	−0.19	−0.27	−0.065	0.51	−0.051	0.19	0.1	0.14	0.38	0.15	0.14
	Midnight blue	0.056	0.22	0.09	0.47	−0.42	−0.02	0.3	0.26	−0.45	−0.37	0.35	0.47	0.34	0.34	0.38	−0.019	0.3	0.41	0.34	0.3
Late Bloom Supermodule	Red brown	−0.56 ★	−0.64 ★★	−0.47	0.31	−0.66 ★★	0.3	−0.62 ★	−0.67 ★★	−0.19	−0.26	0.33	0.38	−0.11	0.26	0.065	−0.6 ★	0.038	0.29	0.075	0.037
	Dark brown	−0.63 ★	−0.62 ★	−0.46	0.53 ★	−0.75 ★★	0.27	−0.53 ★	−0.53 ★	−0.48	−0.62 ★	−0.21	0.21	0.2	0.29	0.55 ★	−0.35	0.5	0.84 ★★	0.5	0.51
	Orange	−0.61 ★	−0.61 ★	−0.48	0.44	−0.81 ★★	0.25	−0.47	−0.61 ★	−0.55 ★	−0.61 ★	0.36	0.61 ★	0.1	0.53 ★	0.42	−0.54 ★	0.39	0.66 ★★	0.4	0.4

Extended Data Fig. 3 | Correlations of Z-score normalized *R. pomeroyi* gene expression module eigengenes with environmental data. Expression was measured by RNAseq after incubation in seawater collected on 14 dates at Monterey Bay Station M0 in Fall, 2016. Dinoflagellate parasites are members of the Syndinales clade. Cells are colored by Pearson's R parameter. Two stars indicate correlations at $p < 0.01$; one star indicates correlations at $p < 0.05$. d.f. = 12.

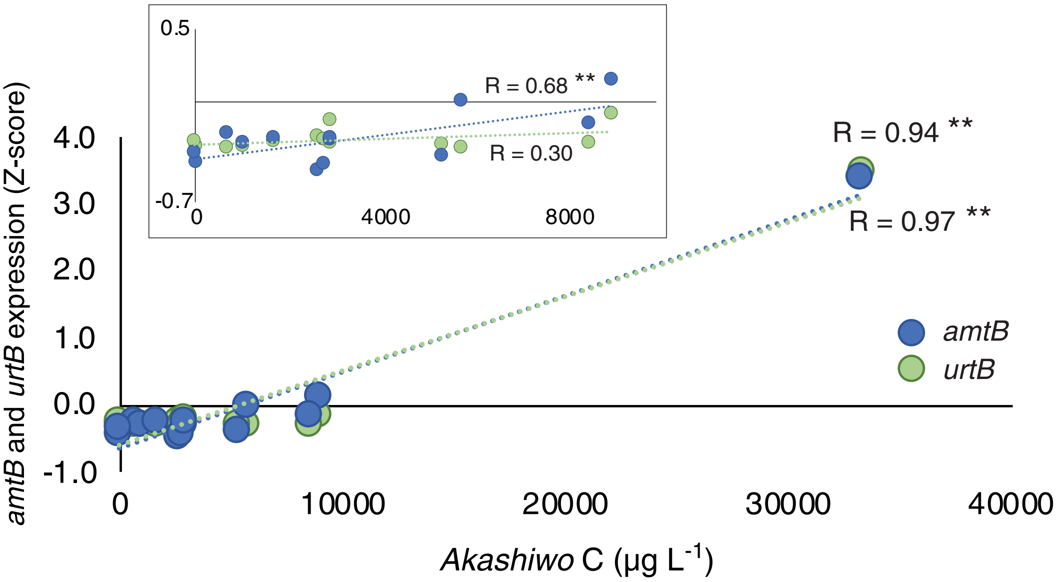

Extended Data Fig. 4 | Correlations of representative *R. pomeroyi* genes for transport of ammonium (*amtB*) and urea (*urtB*) with *Akashiwo* biomass. The extreme value of *Akashiwo* biomass is removed in the inset. **, significant Pearson's R correlation, with $p < 0.001$ for *amtB* and *urtB* in the main figure, d.f. = 12; and $p = 0.010$ for *amtB* and $p = 0.331$ for *umtB* in the inset figure, d.f. = 11.

nature research

Corresponding author(s): Mary Ann Moran

Last updated by author(s): Jun 22, 2020

Reporting Summary

Nature Research wishes to improve the reproducibility of the work that we publish. This form provides structure for consistency and transparency in reporting. For further information on Nature Research policies, see our Editorial Policies and the Editorial Policy Checklist.

Statistics

For all statistical analyses, confirm that the following items are present in the figure legend, table legend, main text, or Methods section.

n/a	Confirmed	
☐	☒	The exact sample size (*n*) for each experimental group/condition, given as a discrete number and unit of measurement
☒	☐	A statement on whether measurements were taken from distinct samples or whether the same sample was measured repeatedly
☐	☒	The statistical test(s) used AND whether they are one- or two-sided *Only common tests should be described solely by name; describe more complex techniques in the Methods section.*
☒	☐	A description of all covariates tested
☒	☐	A description of any assumptions or corrections, such as tests of normality and adjustment for multiple comparisons
☐	☒	A full description of the statistical parameters including central tendency (e.g. means) or other basic estimates (e.g. regression coefficient) AND variation (e.g. standard deviation) or associated estimates of uncertainty (e.g. confidence intervals)
☐	☒	For null hypothesis testing, the test statistic (e.g. *F*, *t*, *r*) with confidence intervals, effect sizes, degrees of freedom and *P* value noted *Give P values as exact values whenever suitable.*
☒	☐	For Bayesian analysis, information on the choice of priors and Markov chain Monte Carlo settings
☒	☐	For hierarchical and complex designs, identification of the appropriate level for tests and full reporting of outcomes
☒	☐	Estimates of effect sizes (e.g. Cohen's *d*, Pearson's *r*), indicating how they were calculated

Our web collection on statistics for biologists contains articles on many of the points above.

Software and code

Policy information about availability of computer code

Data collection	No software was used.
Data analysis	Software used for bioinformatic analysis is described and cited in the methods section of the manuscript; summary: Fastx-toolkit-0.0.14 (read quality filtering) BWA-0.7.15 (read mapping to R. pomeroyi genome) HTSeq-0.9.1 (generate read counts by gene) DESeq2 v1.24.0 (differential gene expression between samples) WGCNA v1.69 (co-expression network analysis of gene expression) GToTree v1.4.1 (phylogenomic tree construction) qiime2-2019 (ASV analysis) R Stats Package v3.6.1 (prcomp function for principal components analysis)

For manuscripts utilizing custom algorithms or software that are central to the research but not yet described in published literature, software must be made available to editors and reviewers. We strongly encourage code deposition in a community repository (e.g. GitHub). See the Nature Research guidelines for submitting code & software for further information.

Data

Policy information about availability of data

All manuscripts must include a data availability statement. This statement should provide the following information, where applicable:

- Accession codes, unique identifiers, or web links for publicly available datasets
- A list of figures that have associated raw data
- A description of any restrictions on data availability

Data that support the findings of this study have been deposited in NCBI SRA with BioProject numbers PRJNA641119 (RNA-seq) and PRJNA511156 - PRJNA511331 (16S and 18S rRNA data), and the Biological and Chemical Oceanography Data Management Office under DOI:10.1575/1912/bco-dmo.756413.2 at https://www.bco-dmo.org/dataset/756413/data (environmental data). The publicly available datasets used were SILVA v132 ribosomal RNA database (https://www.arb-silva.de/documentation/release-132) and Protist Ribosomal Reference (PR2) database (https://pr2-database.org).

Field-specific reporting

Please select the one below that is the best fit for your research. If you are not sure, read the appropriate sections before making your selection.

☐ Life sciences ☐ Behavioural & social sciences ☒ Ecological, evolutionary & environmental sciences

For a reference copy of the document with all sections, see nature.com/documents/nr-reporting-summary-flat.pdf

Ecological, evolutionary & environmental sciences study design

All studies must disclose on these points even when the disclosure is negative.

Study description	A marine bacterium was added into samples from a natural coastal phytoplankton bloom on 14 different dates. After a 90 minute incubation, cells were filtered from the seawater community and analyzed by RNAseq. n = 3 at each date except Sept. 30, n = 2 (lost replicate). Two controls in defined medium were run one time each, n = 3.
Research sample	Samples consisted of marine bacterium Ruegeria pomeroyi mixed with a natural coastal microbial community. R. pomeroyi was chosen because it is a commonly used model organism for studies of heterotrophic marine bacteria, and its full genome was sampled by RNA-Seq. The natural community samples were chosen to be collected from Monterey Bay in the fall season because a fall phytoplankton bloom occurs predictably each year.
Sampling strategy	Sample size for the incubations was 350 ml, chosen to provide sufficient cell material for RNAseq analysis. Incubations were in triplicate as used in current environmental RNASeq analyses to address within-treatment variability within the constraints of library preparation and sequencing costs.
Data collection	Seawater samples were collected from a small boat using a Niskin sampler and returned immediately to a shore laboratory where R. pomeroyi cells were added. Brent Nowinski recorded the data.
Timing and spatial scale	Sampling was conducted from September 28 through October 31 on a 2-3 day schedule as determined by boat availability. Samples were collected from surface seawater (6 m depth). Samples were collected at a single site in Monterey Bay: sampling station MO (36.835 N, 121.901 W).
Data exclusions	No data were excluded.
Reproducibility	Control experiments were run to obtain RNAseq analysis in a defined medium with a known carbon source. In total, 14 addition experiments and 2 control experiments were run. Each set of triplicates analyses was conducted on a different date, with the goal of assessing the unique seawater conditions on each date.
Randomization	Nucleic acid samples were extracted in randomized order.
Blinding	Blinding was not used, as each experiment was performed on a unique date for which seawater conditions (microbial community composition, temperature, salinity, etc.) were also recorded for environmental context.

Did the study involve field work? ☒ Yes ☐ No

Field work, collection and transport

Field conditions	Seawater samples were collected from Monterey Bay during Fall of 2016 on 14 different dates that varied in environmental conditions. A link to publicly available environmental data is provided in the manuscript.
Location	Surface seawater from 6m depth, Station M0, Monterey Bay, CA, USA, 36.835 N, 121.901 W
Access & import/export	Access to Monterey Bay is not controlled.
Disturbance	No disturbance occurred as a result of this study.

Reporting for specific materials, systems and methods

We require information from authors about some types of materials, experimental systems and methods used in many studies. Here, indicate whether each material, system or method listed is relevant to your study. If you are not sure if a list item applies to your research, read the appropriate section before selecting a response.

Materials & experimental systems

n/a	Involved in the study
☒	☐ Antibodies
☒	☐ Eukaryotic cell lines
☒	☐ Palaeontology and archaeology
☒	☐ Animals and other organisms
☒	☐ Human research participants
☒	☐ Clinical data
☒	☐ Dual use research of concern

Methods

n/a	Involved in the study
☒	☐ ChIP-seq
☒	☐ Flow cytometry
☒	☐ MRI-based neuroimaging